2008

Berkovich indentation of diamondlike carbon coatings on silicon substrates

Ayesha J. Haq
University of Wollongong, ayesha@uow.edu.au

Paul Munroe
University of New South Wales

Mark Hoffman
University of New South Wales, m.hoffman@unsw.edu.au

Phil Martin
CSIRO, Phil.Martin@csiro.au

Avi Bendavid
CSIRO, Avi.Bendavid@csiro.au

Berkovich indentation of diamondlike carbon coatings on silicon substrates

Abstract

The deformation behavior of diamondlike carbon (DLC) coatings on silicon substrates induced by Berkovich indentation has been investigated. DLC coatings deposited by a plasma-assisted chemical vapor deposition technique were subjected to nanoindentation with a Berkovich indenter over a range of maximum loads from 100 to 300 mN. Distinct pop-ins were observed for loads greater than 150 mN. However, no pop-out was observed for the loads studied. The top surface of the indents showed annular cracks with associated fragmented material. The cross sections showed up to 20% localized reduction in thickness of the DLC coating beneath the indenter tip. Cracking, {111} slip, stacking faults, and localized phase transformations were observed in the silicon substrate. The discontinuities in the load-displacement curves at low loads are attributed to plastic deformation of the silicon substrate, whereas at higher loads they are attributed to plastic deformation as well as phase transformation.

Keywords

berkovich, coatings, diamondlike, indentation, silicon, carbon, substrates

Disciplines

Engineering | Science and Technology Studies

Publication Details

Haq, A. J., Munroe, P. R., Hoffman, M., Martin, P. J. & Bendavid, A. 2008, 'Berkovich indentation of diamondlike carbon coatings on silicon substrates', Journal of Materials Research, vol. 23, no. 7, pp. 1862-1869.

Berkovich indentation of diamondlike carbon coatings on silicon substrates

Ayesha J. Haq,[a] P.R. Munroe, and M. Hoffman
School of Materials Science and Engineering, University of New South Wales, Sydney, NSW 2052, Australia

P.J. Martin and A. Bendavid
Commonwealth Scientific and Industrial Research Organization (CSIRO) Materials Science and Engineering, Lindfield, NSW 2070, Australia

(Received 28 September 2007; accepted 24 January 2008)

The deformation behavior of diamondlike carbon (DLC) coatings on silicon substrates induced by Berkovich indentation has been investigated. DLC coatings deposited by a plasma-assisted chemical vapor deposition technique were subjected to nanoindentation with a Berkovich indenter over a range of maximum loads from 100 to 300 mN. Distinct pop-ins were observed for loads greater than 150 mN. However, no pop-out was observed for the loads studied. The top surface of the indents showed annular cracks with associated fragmented material. The cross sections showed up to 20% localized reduction in thickness of the DLC coating beneath the indenter tip. Cracking, {111} slip, stacking faults, and localized phase transformations were observed in the silicon substrate. The discontinuities in the load–displacement curves at low loads are attributed to plastic deformation of the silicon substrate, whereas at higher loads they are attributed to plastic deformation as well as phase transformation.

I. INTRODUCTION

Diamondlike carbon (DLC) coatings are metastable amorphous films composed of a mixture of sp^2-graphite and sp^3-diamond hybridized structures in various proportions. Their unique combination of properties such as extremely high hardness, elastic modulus, low friction coefficients, high chemical inertness, good wear resistance, and excellent corrosion resistance make them attractive for applications such as cutting tools, razor blades, magnetic recording heads, storage devices, and applications in the biomedical industry.[1–3]

Nanoindentation has been extensively used for evaluating the mechanical properties and deformation behavior of DLC coatings.[4–17] A large number of these investigations have focused on the effect of various deposition techniques and parameters of deposition on the structure and mechanical properties of the coatings.[6–10] The effect of film thickness has been studied by Beake and Lau.[11] Moreover, the effect of substrate type on the mechanical behavior of DLC coatings has been investigated by Steadler and Schiffman,[12] Poliakov et al.,[13] and Zhang and Huang.[14] Surface characterization techniques such as scanning electron microscopy (SEM) and atomic force microscopy (AFM) have been used by Bhushan et al.,[3–5] Chowdhury et al.,[9,10] and Xu and Rowcliffe[15] to investigate the cracking and deformation of DLC coatings. Based on the surface morphology of the indents, Bhushan et al.[3–5] have related the observed discontinuities during loading, i.e., the pop-ins, in the load–displacement curves of thin DLC coatings on silicon to the through-thickness cracks in the coating. Further, they have attributed the discontinuity on unloading, i.e., the pop-out to the formation of lateral cracks. In contrast, Beake and Lau[11] have ascribed the pop-out to the phase transformations that occur in the silicon substrate based on available literature on nanoindentation studies of pristine silicon, since it is well known that phase transformations occur during loading (from Si-I to Si-II) and unloading (Si-II to Si-III/Si-XII), resulting in discontinuities in the load–displacement curves.[18–23] However, these authors have not presented any evidence of the subsurface microstructures by examining cross sections through the indents. On the other hand, Michler and Blank[16] have identified the preferential locations for initiation of cracks and have presented evidence of surface as well as interface cracks in DLC coatings on steel substrates. However, there have been no systematic studies on the deformation behavior following Berkovich indentation of DLC coatings on silicon substrates involving the examination of cross sections of the deformed coatings, and consequently, no investigations relating the indentation

[a]Address all correspondence to this author.
e-mail: ayesha@materials.unsw.edu.au
DOI: 10.1557/JMR.2008.0232

behavior to the observed subsurface structure of the coatings. This has been primarily due to the difficulty in the preparation of cross-sectional thin foils for transmission electron microscopy (TEM) through localized regions in the vicinity of indentations.

In recent years, examination of subsurface microstructures has become possible due to the emergence of focused ion beam (FIB) technology as a tool for cross-sectional TEM (XTEM) sample preparation.[24,25] Using this technique in a recent investigation, we have correlated the XTEM observations with the spherical indentation behavior of DLC coatings on silicon (100) substrates.[26] Unlike the spherical indenter, which produces a more uniform stress field under the indenter, the stress gradients and therefore the damage induced by a Berkovich indenter, which possesses a pointed tip, is both different and more severe.[20] This is likely to result in a complex deformation behavior below the indenter. However, no XTEM studies involving the deformation behavior of DLC coatings on silicon substrates following indentation with a Berkovich indenter have been reported.

Therefore, in this study, the microstructural changes resulting from deformation induced by a Berkovich indenter were investigated in DLC coatings on (100) silicon substrates deposited by a radio frequency plasma-assisted chemical vapor deposition (PACVD) technique. In this paper, emphasis is placed on the response of the silicon substrate to contact loading. Following nanoindentation, the deformed regions were examined by SEM, FIB, and XTEM. The observed microstructural features were correlated to the load–displacement behavior, and the results were compared with those obtained earlier on the same coating with a spherical indenter of 5-μm radius.[26]

II. EXPERIMENTAL PROCEDURE

DLC coatings containing hydrogen were deposited onto (100) silicon substrates using a radio frequency (rf) PACVD technique. The chamber was evacuated to a pressure of approximately 2×10^{-5} mbar. Prior to deposition, the substrates were in situ sputter cleaned for 5 min in argon plasma operated at 25 mTorr with the argon flow rate set at 10 sccm at 200 W power, and self bias was about 650 V. To improve the adhesion, a thin layer of hydrogenated amorphous silicon carbide (a:SiCH) was first deposited onto the substrate using tetramethylsilane (TMS) as precursor. The interlayer deposition was performed at 25 mTorr with the TMS flow rate set at 85 sccm at 200 W power for 3 min. For the deposition of the hydrogenated amorphous carbon (a-C:H) layer, acetylene gas was introduced at a flow rate of 100 sccm into the chamber, and the pressure and power were set to 50 mT and 200 W respectively for 10 min.

The composition of the coating was determined by visible Raman spectroscopy, which was carried out using a Renishaw Raman Spectroscope 2000 (Gloucestershire, UK) at an excitation wavelength of 514 nm with an Ar laser of spot size 5 μm. After background subtraction, the Raman spectra were fitted with two Gaussians and the peak parameters (G and D peak positions and the intensity ratio I_D/I_G) were determined.[27,28] Microstructural characterization of the as-deposited coatings was carried out by both FIB and XTEM, as described elsewhere.[26]

The coatings were subjected to nanoindentation with a Berkovich indenter to various maximum loads between 100 and 300 mN using the UMIS-2000 (Ultra Micro-Indentation System) [CSIRO, Australian Scientific Instruments (ASI) Pty. Ltd., Australia]. Arrays of ten indents were performed at each load with a spacing of 50 μm between indents. For indentation to loads of 100 and 150 mN, 50 increments were recorded during loading and unloading, whereas 100 increments were used for higher loads. The unloading rates ranged from 1 to 2 mN/s. Subsequently, a Nova Nanolab 200 dual beam FIB (FEI, North America NanoPort, OR) was used for imaging the residual indents as well as for preparing and imaging cross sections through the indentations. XTEM specimens were prepared from the indents using the Nova Nanolab 200 dual-beam FIB, and the samples were lifted out onto C-coated copper grids using an optical microscope and a glass needle attached to a piezoelectric device. The thin foils were examined normal to the ⟨110⟩ of the silicon substrate in a Philips CM200 TEM.

III. RESULTS AND DISCUSSION

The as-deposited DLC coating had a featureless appearance consistent with its amorphous nature. From FIB and XTEM examination, the thickness of the coating was determined to be 1.6 μm. XTEM also revealed the presence of a 40-nm-thick a:SiCH layer at the interface.[26] The visible Raman spectrum (Fig. 1) shows a prominent G peak and a shoulder D peak, features characteristic of DLC coatings.[27,29] By fitting the spectrum with two Gaussians, the G peak position and the area ratio of the intensities of the two peaks I_D and I_G were quantified as 1556 cm^{-1} and 1.4, respectively. Through comparison of these values with the empirical plots given by Ferrari and Robertson,[27] the total sp^3 content (including C–H bonds) of the coating was estimated to be in the range of 30–35%. From the measured slope of the photoluminescence background of the spectrum and using the formula given by Casiraghi et al.,[28] the hydrogen content of the film was calculated as ~28 at.%.

The load–displacement curves obtained on indentation of the coatings to various maximum loads up to 300 mN using a Berkovich indenter are shown in Fig. 2(a). The coating exhibits significant elastic recovery during unloading, consistent with earlier studies.[26,30] The maximum and residual depths of penetration, as well as the

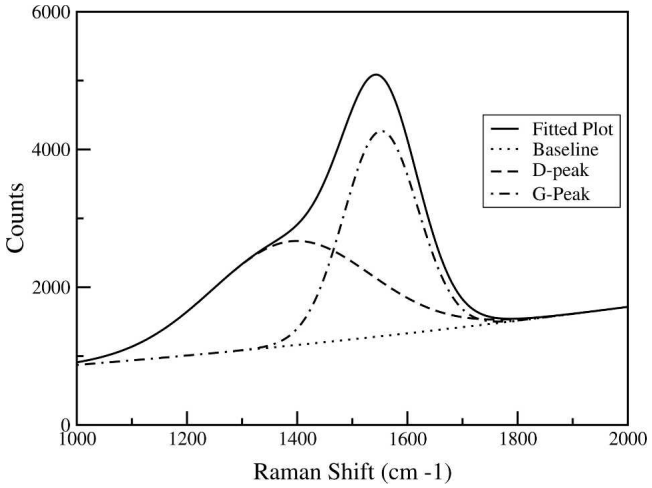

FIG. 1. Visible Raman spectrum from the DLC coating showing the fitted peak and the deconvoluted G and D peaks.

degree of recovery, increased with the maximum load. Figure 2(b) shows a comparison between the maximum and residual depths of penetration and the degree of recovery obtained in this study with that obtained earlier on indentation of the DLC coating of the same thickness with a spherical indenter having a tip radius of 5 μm.[26] For the range of loads studied here, the total and residual depths of penetration appear to vary almost linearly with load for both types of indenters. Further, for a given load, the maximum and the residual depths of penetration obtained during Berkovich indentation are over 10% higher than those obtained on indentation with a spherical indenter consistent with the expected behavior for a sharper Berkovich indenter. However, the magnitude of recovery, which is ~60%, is almost the same for both indenter types.

For maximum indentation loads of 150 mN, the load–displacement curves [Fig. 2(a)] displayed a small discontinuity at loads close to the maximum load used. However, following indentation to 200 mN, this discontinuity become clearly evident. It can be observed that a small pop-in occurs in the load range of 140–160 mN. As noted earlier, 10 indentations were performed at each load. Thus there is some scatter in the load at which the pop-ins are observed. With increase in maximum indentation load to 250 mN, another pop-in appeared in the range 180–210 mN; with further increase in load to 300 mN, a third pop-in was observed in the range 240–260 mN. Although higher penetration depths are obtained in Berkovich indentation, the loads at which pop-ins appear, for a given maximum load, are generally similar to those observed during indentation with a spherical indenter.[26] Further, a clear pop-out was not observed at the range of loads studied, as was the case with spherical indentation of the same material.

The size of the residual indents for Berkovich indentation was quantified in terms of the contact edge AB, which is shown in a secondary electron image [Fig. 3(a)] of the top surface of the indent for a 300 mN indent. The length AB of the residual indents increased from ~4 μm at 100 mN to ~8 μm at 300 mN [Fig. 3(a)]. No cracks were evident on the indent surface on indentation to maximum loads below 150 mN. On increasing the indentation load to 200 mN, some indents showed annular cracks (also referred to as picture frame cracks) and locally fragmented material within them. The incidence of cracking increased with further increases in load, and at

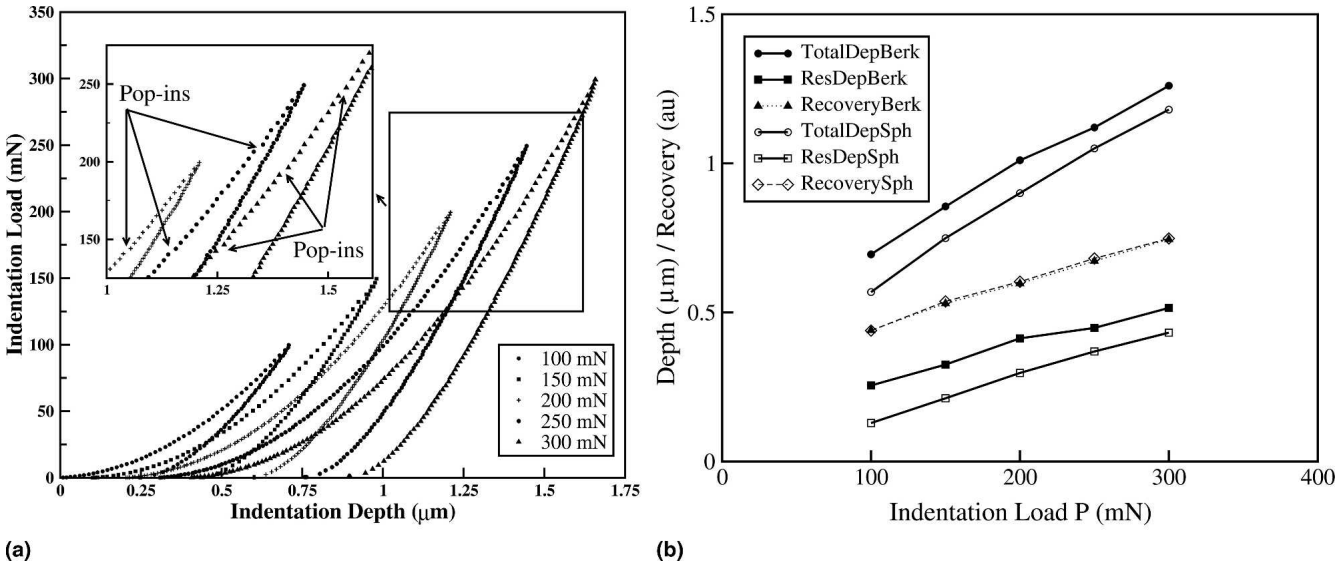

FIG. 2. (a) Load–displacement curves at various maximum loads. The curves have been plotted with an offset of 0.1, 0.2, 0.3, and 0.4 μm on the *x* axis for maximum loads of 150, 200, 250, and 300 mN, respectively. (inset) Magnified view of the boxed region. (b) Plot showing the comparison of the total and residual depth of penetration and recovery for Berkovich and spherical indentation on DLC coatings.[26]

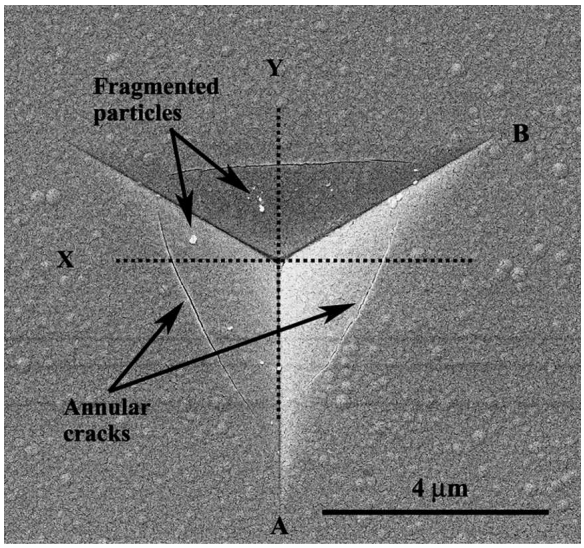

(a)

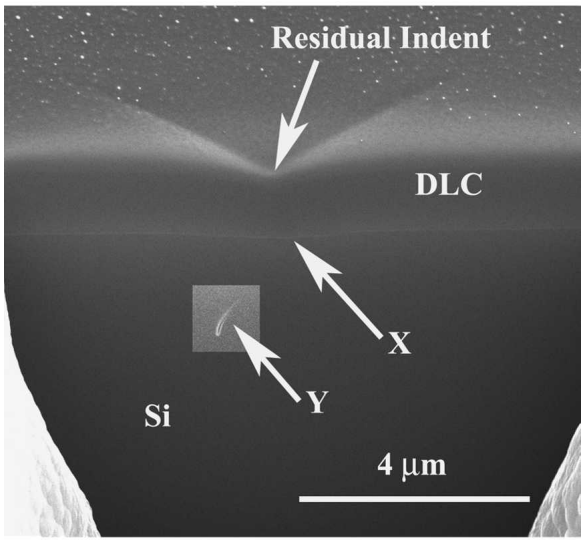

(b)

FIG. 3. Secondary electron images (from FIB) after indentation to 300 mN: (a) top surface showing annular cracks and fragmented material and (b) cross section showing bending at the interface (X) and the median crack (Y) below the indent. The contrast has been enhanced to make the crack more visible.

300 mN [Fig. 3(a)] most of the indents showed annular cracking. However, no radial cracks developed at the indentation corners, even at a load of 300 mN.

Because the Berkovich indenter has an asymmetrical shape, FIB cross sections, as well as XTEM specimens, through the indents at all the loads were prepared along two orientations designated X and Y [Fig. 3(a)]. However, for comparison purposes, most of the images shown in this study correspond to orientation Y, except for the 250 mN indent (Fig. 8). Secondary electron FIB imaging of the cross sections of the indents at all loads showed a localized reduction in the thickness of the coating in the region just below the indenter tip, as compared to an unindented region, indicating that the coating undergoes localized plastic compression in the direction of loading. This compression, which was a maximum at the indenter tip, increased with load without any observation of radial or lateral cracks in the coating or delamination at the coating–substrate interface. These observations are similar to the results with a spherical indenter, except that the localized compression at the indenter tip is significantly higher than that observed with a spherical indenter, which is in agreement with the larger depths of penetration observed in the load–displacement curves. For loads above 150 mN, the interface showed evidence of bending, the magnitude of which increased with load. On indentation to the maximum load of 300 mN [Fig. 3(b)], substantial bending at the interface (labeled X), as well as a median crack (marked Y) in the substrate, is clearly evident. Further, it can be seen from Fig. 3(b) that the annular cracks observed on the surface [Fig. 3(a)] do not appear to extend through the thickness of the coating, consistent with earlier observations on steel substrates[16] as well as on silicon substrates.[26]

Figure 4 shows a bright-field XTEM image of the cross section of coating following indentation to a maximum load of 100 mN. The coating clearly reveals localized plastic deformation of the DLC coating below the indenter tip in the direction of loading without any cracking, consistent with the observations using spherical indenter[26] and that reported by simulation studies.[31] From the difference in the thickness of the coating at AB and CD the maximum plastic compression of the coating was measured as ~10%. This value, which is more than double the amount of deformation (~4.5%) reported earlier[26] for indentation to the same load on a coating of similar thickness with a spherical indenter, indicates the ability of the coating to undergo substantial localized deformation without cracking, even with a sharper indenter.

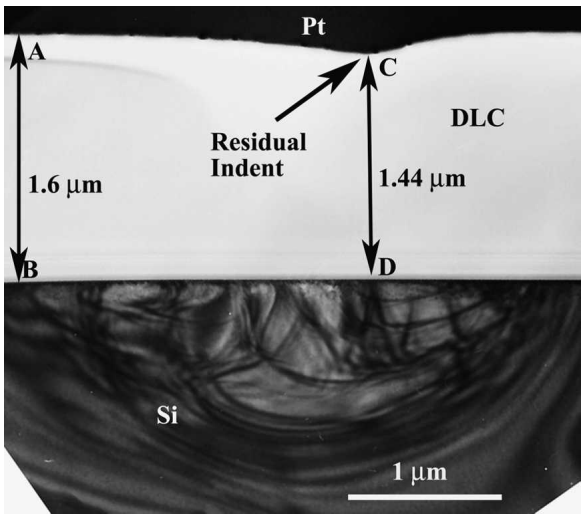

FIG. 4. Bright-field XTEM micrograph after indentation to 100 mN load.

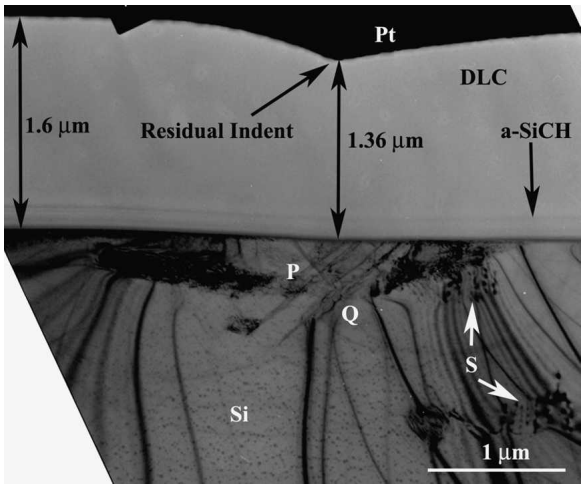

FIG. 5. Bright-field XTEM micrograph after indentation to 150 mN load showing narrow slip bands (P, Q) and threading dislocations (S).

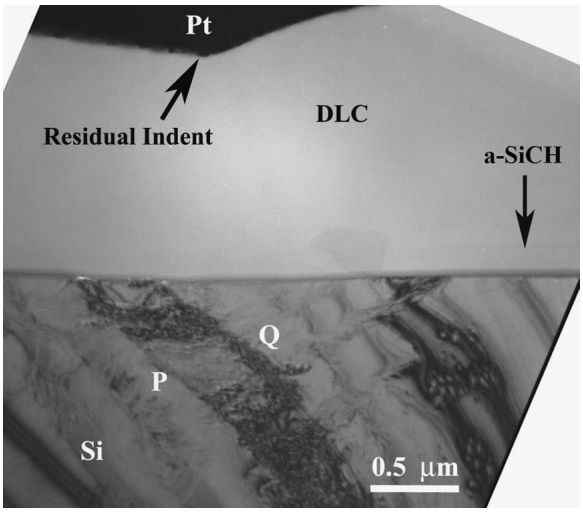

FIG. 6. Bright-field XTEM micrograph showing slip bands (P, Q) after indentation to a load of 200 mN.

The observed localized deformation is a consequence of the development of highly localized stresses beneath the sharper Berkovich indenter, which also resulted in the larger penetration depths. Although the coating exhibits substantial localized deformation, there is no corresponding bending at the interface nor any plastic deformation in the substrate, which showed only some bend contours, indicating that the coating is able to support the applied load without transferring substantial load to the substrate. Consequently, the corresponding load–displacement curve [Fig. 2(a)] shows no discontinuities during loading.

On increasing the indentation load to 150 mN, the maximum compressive strain in the coating in the loading direction increased to ~15% (at the tip), again without any cracking or delamination (Fig. 5). However, at this load, plastic deformation was evident in the substrate confined to a small region beneath the indenter tip. Narrow slip bands (marked P, Q) are observed, which are inclined at an angle of 54° to the (100) surface, indicating that they are aligned on the {111} planes, which are the preferential slip planes for the diamond cubic Si-I phase. These bands extend to a depth of only 0.8 μm within the substrate and form a characteristic V shape. A few threading dislocations (marked S) perpendicular to the interface, i.e., lying parallel to [100], are also seen. The extent of deformation of the substrate is similar to that seen during spherical indentation of these coatings.[26] The load–displacement curves [Fig. 2(a)] show small pop-ins within a load range around 150 mN, which are presumably associated with the onset of slip.

The localized compressive strain in the coating increased to ~17% with increase in the indentation load to 200 mN (Fig. 6). The substrate consequently shows significant deformation with coarse slip bands (labeled P, Q) on {111} planes that extend to about 1.5 μm from the interface and a high density of dislocations but without concomitant phase transformation similar to the results on spherical indentation.[26] A small number of twins were also observed in cross sections prepared along the X orientation. However, a higher density of defects was also observed following loading to 250 mN, as described later and shown in Fig. 8. Although the coating still remained free of cracks, delamination is clearly evident in small regions where slip bands intersect the interface. The corresponding load–displacement curve [Fig. 2(a)] exhibited a distinct pop-in. In earlier studies on thinner (400 nm) DLC coatings, based on surface characterization techniques, pop-ins have been related to the formation of through thickness cracks in the coatings,[4,5] whereas in uncoated silicon the pop-ins have been attributed to phase transformations.[19–23] However, in this case, neither phase transformation in silicon nor any through-thickness cracks in the coating have been observed. This is a consequence of the altered loading conditions arising due to the presence of the DLC coating above the silicon and can be explained using the schematic illustration shown in Fig. 7. During indentation, uncoated silicon [Fig. 7(a)] experiences high hydrostatic stresses in a localized region beneath the indenter tip. These localized stresses are sufficient to initiate transformation in small volumes of the material.[19] On the other hand, in the case of the DLC coating [Fig. 7(b)], there is a distribution of the applied load over a much larger area of the silicon substrate, which effectively decreases the local stress concentration beneath the indenter to values insufficient for phase transformations to occur. This redistribution of stresses, however, appears to have resulted in a larger volume of silicon undergoing dislocation motion, sufficient to produce a pop-in event in the loading curve.

Indentation to a maximum load of 250 mN further increased the compressive plastic strain in the coating to ~18%. The plastic deformation in the substrate also

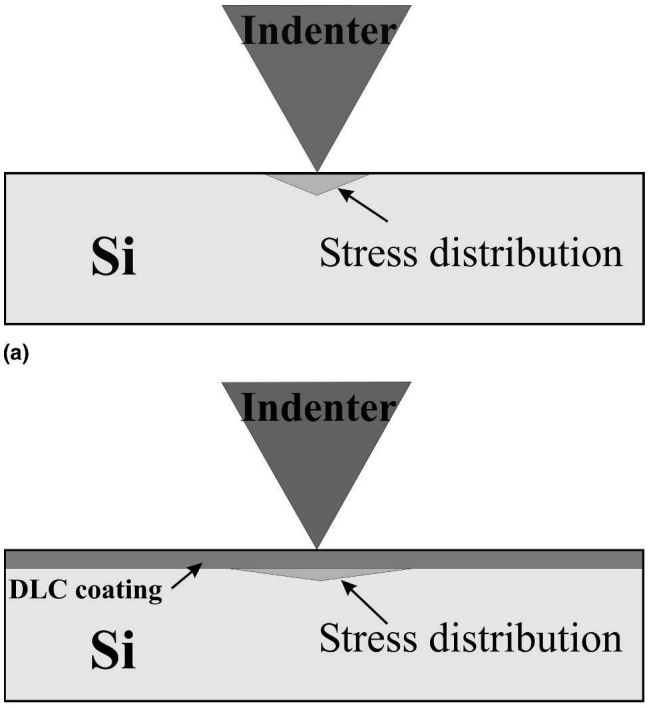

FIG. 7. Schematic representation of hydrostatic stresses beneath the indenter tip: (a) uncoated silicon and (b) DLC coating on silicon.

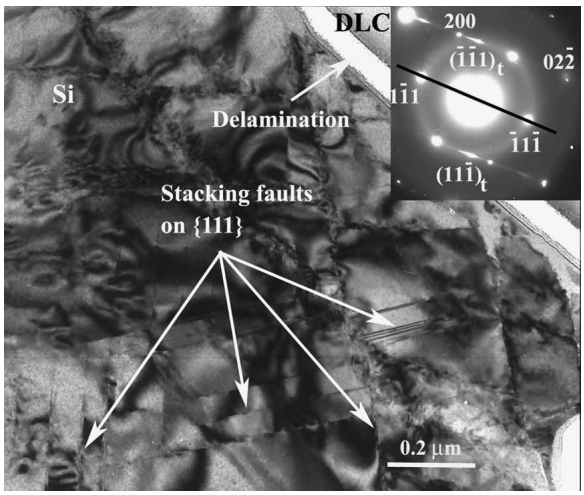

FIG. 8. Bright-field TEM micrographs at a load of 250 mN showing stacking faults on {111} planes and delamination at the interface. Inset shows extra reflections (labeled with subscript t) and streaking along [111] direction.

increased, as shown in Fig. 8, which shows a bright-field TEM image of the cross section through an indent corresponding to the X orientation of Fig. 3(a). Stacking faults on {111} planes of silicon (marked X) are visible, and correspondingly, extra reflections and streaking along [111] direction, both associated with stacking faults and twinning, are seen in the selected area diffraction pattern from this region (inset). However, still there is no evidence of phase transformation at this load. Although the coating did not develop any through-thickness cracks, delamination (marked Y) beneath the indenter is clearly evident. Similar to the case of spherical indentation,[26] this delamination was found to occur in the TEM sample preparation stage in the process of relieving the high residual stresses known to be present in the coating.[32] In the absence of any phase transformation, the pop-ins in the load–displacement curve can be attributed to the deformation mechanism operating in the substrate.

A further increase in load to 300 mN increased the local compressive plastic strain of the coating to ~20%,

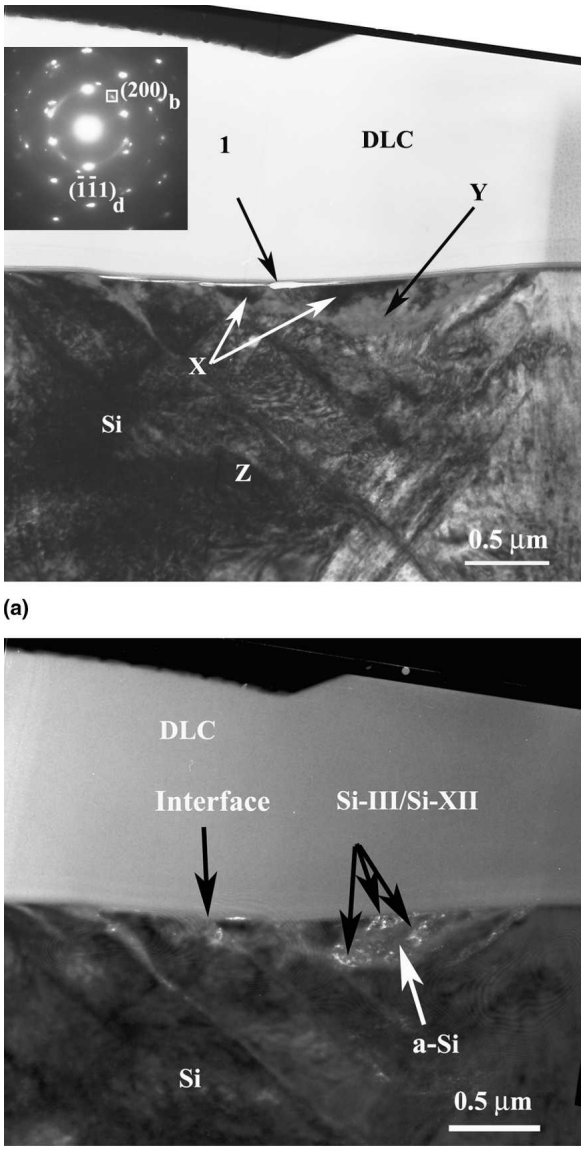

FIG. 9. Bright-field TEM micrographs at a load of 300 mN showing (a) plastic deformation in the coating as well as the substrate and the transformation zone beneath the indenter tip. (inset) SAD pattern from the transformation zone. (b) Dark-field image taken using the boxed reflection in (a) showing the crystalline phases.

resulting in significant bending at the DLC-a:SiCH interface [Fig. 9(a)]. Although the cross section of the coating is still free of cracks, delamination in the area directly below the indentation (marked 1) is seen. Also, there is extensive deformation in the substrate and some twinning is visible, but it is masked by contrast from the high density of dislocations. Further, a shallow, ~350–400 nm thick, hemispherical phase transformation zone labeled Y is observed, which displays a contrast distinct from that of the bulk crystalline silicon, labeled Z. The diffraction pattern from this zone (inset) displayed strong rings corresponding to the amorphous silicon as well as additional reflections consistent with the presence of high-pressure phases, BC8 (Si-III) and R8 (Si-XII). These observations are similar to those reported for uncoated silicon at loads as low as 30 mN[21,22] as well for DLC coatings following spherical indentation to similar loads.[26] A dark-field micrograph [Fig. 9(b)], taken using the boxed reflection, shows the presence of crystalline phases in the transformation zone. However, the amount of crystalline BC8/R8 phases is much smaller than that of the amorphous phase. This can be attributed to the loads insufficient for complete transformation due to the wider distribution of load by the DLC coating.

The additional pop-in in the load–displacement curve [Fig. 2(a)] can be attributed to the occurrence of transformation of Si-I to Si-II. However, this transformation has not resulted in an elbow or pop-out in the corresponding unloading curve [Fig. 2(a)]. These results are similar to our earlier results obtained with a spherical indenter but inconsistent with those reported on uncoated silicon.[21–23] However, recent studies on uncoated silicon[18] have reported that such phase transformations do not necessarily result in pop out events. Another reason that can be attributed to the absence of a pop-out is the presence of more of the amorphous silicon than the crystalline phases [Fig. 9(b)]. In uncoated silicon, formation of a-Si has been shown to give rise to a gradual expansion in the lattice resulting in gradual indenter uplift, thereby slowing down the upward movement of the indenter. In this study, due to the presence of DLC layer above the silicon, some of the expansion due to the transformation of Si-II is partially accommodated in the coating, reducing the extent of uplift of the indenter and thereby resulting in the absence of a pop-out.

The transformation zone observed in this study is hemispherical (Fig. 9) as against the triangular or pyramidal shape observed during Berkovich indentation of uncoated silicon.[20,33] Although the coating experiences loading from a pointed indenter, it distributes the stresses over a larger volume of the silicon substrate. Therefore, the substrate experiences a loading condition similar to that of a spherical indenter instead of a pointed indenter and hence develops a hemispherical transformation zone.

Further, similar to the observations with a spherical indenter, a small amount of untransformed Si-I is observed in the region X between the interface and the transformation zone. Most of the results on uncoated silicon have not indicated the presence of untransformed Si-I directly beneath the indenter tip, and so this again may be a consequence of incomplete transformation of Si-I to Si-II due to the altered loading condition brought about by the presence of the DLC coating above the silicon. Unlike the observations in uncoated silicon, the presence of defects over large areas outside the vicinity of the indentation, both parallel to the interface as well as within the bulk of the substrate, is a further indication of the redistribution of stresses.

The pressures induced by sharp Berkovich indenters are larger than those developed by spherical indenters. Accordingly, the coatings exhibit larger penetration depths, which are manifested in a substantially larger magnitude of localized plastic compression of the coating, as shown in the XTEM images. The deformation mechanisms observed in the silicon substrate, however, appear to be similar for both types of indentation, i.e., the maximum applied load (150 mN) at which slip initiates and the load at which the induced phase transformation is observed in the substrate (300 mN) are the same for the loads up to 300 mN. This is because the DLC coating accommodates the localized stresses generated by the sharper tip by inducing deformation over a substantially larger area of the substrate without cracking. Therefore, the effective stresses transferred to the substrate in Berkovich indentation appear similar to those seen in spherical indentation.

IV. CONCLUSIONS

Berkovich indentation of the DLC coating resulted in a substantially larger magnitude of compressive plastic strain in the direction of loading as compared to a spherical indenter. This compression, which was a maximum at the tip, increased from ~10% at 100 mN to 20% at 300 mN without any observation of radial cracks or lateral cracks in the coating. Pop-ins appeared for maximum loads of 150 mN and above, but no pop-outs were evident. Annular cracks observed on the surface did not extend through the thickness of the coating. For loads above 150 mN, XTEM revealed dislocations, stacking faults, and slip bands on {111} planes of the silicon substrate, the extent of deformation increasing with load. On indentation to 300 mN, a phase transformation zone, containing both amorphous silicon and Si-III and Si-XII, was observed.

The discontinuities in the load–displacement curves have been correlated with the observed microstructural features, i.e., the pop-ins observed at the loads of 250 mN and below are attributed to the plastic deformation of the silicon substrate through dislocation motion and

formation of stacking faults and at higher loads to phase transformation of the substrate and associated sudden volume reduction. The absence of a distinct pop-out at 300 mN is a result of the formation of a larger amount of a-Si in the transformation zone combined with the accommodation of the associated expansion in lattice by deformation within the DLC coating.

The differences in the microstructures observed with respect to those on uncoated silicon are attributed to the altered stress state in the silicon substrate brought about by the distribution of the applied load by the DLC coating.

ACKNOWLEDGMENT

The authors acknowledge the Australian Research Council for providing financial support.

REFERENCES

1. A.H. Lettington: Applications of diamond-like carbon thin films. *Carbon* **36,** 555 (1998).
2. A. Grill and V. Patel: Tribological properties of diamond-like carbon and related materials. *Diamond Relat. Mater.* **2,** 597 (1993).
3. B. Bhushan: Chemical, mechanical and tribological characterization of ultra-thin and hard amorphous carbon coatings as thin as 3.5 nm: Recent developments. *Diamond Relat. Mater.* **8,** 1985 (1999).
4. X. Li, D. Diao, and B. Bhushan: Fracture mechanisms of thin amorphous carbon films in nanoindentation. *Acta Mater.* **45,** 4453 (1997).
5. X. Li and B. Bhushan: Measurement of fracture toughness of ultra-thin amorphous carbon films. *Thin Solid Films* **315,** 214 (1998).
6. J.C. Sanchez-Lopez, C. Donnet, J.L. Loubet, M. Belin, A. Grill, V. Patel, and C. Jahnes: Tribological and mechanical properties of diamond-like carbon prepared by high-density plasma. *Diamond Relat. Mater.* **10,** 1063 (2001).
7. H. Tojo, Y. Mokuno, A. Chayahara, S. Iura, H. Kasai, N. Toyohara, T. Hidaka, S. Isogawa, M. Hijino, and Y. Horino: Properties of diamond like carbon films by plasma based ion implantation and deposition method applied radio frequency wave and negative high voltage pulses through single feedthrough. *Nucl. Instrum. Methods Phys. Res., Sect. B* **206,** 717 (2003).
8. Y.S. Zou, W. Wang, G.H. Song, H. Du, J. Gong, R.F. Huang, and L.S. Wen: Influence of the gas atmosphere on the microstructure and mechanical properties of diamond-like carbon films by arc ion plating. *Mater. Lett.* **58,** 3271 (2004).
9. S. Chowdhury, M.T. Laugier, and I.Z. Rahman: Effect of target self-bias voltage on the mechanical properties of diamond-like carbon films deposited by RF magnetron sputtering. *Thin Solid Films* **468,** 149 (2004).
10. S. Chowdhury, M.T. Laugier, and I.Z. Rahman: Characterization of DLC coatings deposited by rf magnetron sputtering. *J. Mater. Process. Technol.* **153–154,** 804 (2004).
11. B.D. Beake and S.P. Lau: Nanotribological and nanomechanical properties of 5–80 nm tetrahedral amorphous carbon films on silicon. *Diamond Relat. Mater.* **14,** 1535 (2005).
12. T. Staedler and K. Schiffmann: Correlation of nanomechanical and nanotriboligical behavior of thin DLC coatings on difference substrates. *Surf. Sci.* **482–485,** 1125 (2001).
13. V.P. Poliakov, C.J. de M. Siqueira, W. Veiga, I.A. Hummelgen, C.M. Lepienski, G.G. Kirpilenko, and S.T. Dechandt: Physical and tribological properties of hard amorphous DLC films deposited on difference substrates. *Diamond Relat. Mater.* **13,** 1511 (2004).
14. T.H. Zhang and Y. Huan: Nanoindentation and nanoscratch behaviors of DLC coatings on different steel substrates. *Compos. Sci. Technol.* **65,** 1409 (2005).
15. Z. Xu and D. Rowcliffe: Nanoindentation on diamond-like carbon and alumina coatings. *Surf. Coat. Technol.* **161,** 44 (2002).
16. J. Michler and E. Blank: Analysis of coating fracture and substrate plasticity induced by spherical indenters: Diamond and diamond-like carbon layers on steel substrates. *Thin Solid Films* **381,** 119 (2001).
17. R.K. Singh, M.T. Tilbrook, Z.H. Xie, A. Bendavid, P. Martin, P.R. Munroe, and M. Hoffman: Contact damage evolution in diamondlike-carbon coatings on ductile substrates. *J. Mater. Res.* **23,** 27 (2008).
18. T. Juliano, V. Domnich, and Y. Gogotsi: Examining pressure-induced phase transformations in silicon by spherical indentation and Raman spectroscopy. *J. Mater. Res.* **19,** 3099 (2004).
19. J.E. Bradby, J.S. Williams, J. Wong-Leung, M.V. Swain, and P. Munroe: Transmission electron microscopy observation of deformation microstructure under spherical indentation in silicon. *Appl. Phys. Lett.* **77,** 3749 (2000).
20. J.E. Bradby, J.S. Williams, J. Wong-Leung, M.V. Swain, and P. Munroe: Mechanical deformation in silicon by micro-indentation. *J. Mater. Res.* **16,** 1500 (2001).
21. I. Zarudi and L.C. Zhang: Structure changes in monocrystalline silicon subjected to indentation-experimental findings. *Tribol. Int.* **32,** 701 (1999).
22. I. Zarudi, L.C. Zhang, and M.V. Swain: Microstructure evolution in monocrystalline silicon in cyclic microindentations. *J. Mater. Res.* **18,** 758 (2003).
23. V. Domnich and Y. Gogotsi: Phase transformations in silicon under contact loading. *Rev. Adv. Mater. Sci.* **3,** 1 (2002).
24. J.M. Cairney, P.R. Munroe, and M. Hoffman: The application of focused ion beam technology to the characterization of coatings. *Surf. Coat. Technol.* **198,** 165 (2005).
25. J.M. Cairney, R.D. Smith, and P.R. Munroe: Transmission electron microscope specimen preparation of metal matrix composites using the focussed ion beam miller. *Microsc. Microanal.* **6,** 452 (2000).
26. A.J. Haq, P.R. Munroe, M. Hoffman, P.J. Martin, and A. Bendavid: Nanoindentation-induced deformation behavior of diamond-like carbon coatings on silicon substrates. *Thin Solid Films* **515,** 1000 (2006).
27. A. Ferrari and J. Robertson: Interpretation of Raman spectra of disordered and amorphous carbon. *J. Phys. Rev. B* **61,** 14095 (2000).
28. C. Casiraghi, F. Piazza, A.C. Ferrari, D. Grambole, and J. Robertson: Bonding in hydrogenated diamond-like carbon by Raman spectroscopy. *Diamond Relat. Mater.* **14,** 1098 (2005).
29. M.A. Tamor and W.C. Vassell: Raman "fingerprinting" of amorphous carbon films. *J. Appl. Phys.* **76,** 3823 (1994).
30. N. Savvides and T.J. Bell: Microhardness and Young's modulus of diamond and diamondlike-carbon films. *J. Appl. Phys.* **72,** 2791 (1992).
31. A.M. Stoneham, P.D. Godwin, A.P. Sutton, and S.J. Bull: Elastic and plastic deformation of diamondlike carbons. *Bull. Appl. Phys. Lett.* **72,** 3142 (1998).
32. X.L. Peng and T.W. Clyne: Mechanical stability of DLC films on metallic substrates: Part I-Film structure and residual stress levels. *Thin Solid Films* **312,** 207 (1998).
33. I. Zarudi, L.C. Zhang, W.C.D. Cheong, and T.X. Yu: The difference of phase distributions in silicon after indentation with Berkovich and spherical indenters. *Acta Mater.* **53,** 4795 (2005).